Published by JScE as Proceedings of 4th International Conference on Earthquake Engineering and Post-Disaster Reconstruction Planning (ICEE-PDRP), 19-21 Jan. 2026, Bhaktapur, Nepal

OUT-OF-PLANE DYNAMIC SHOCK TABLE TESTING OF A MOCK-UP UNREINFORCED STONE MASONRY BUILDING

Marc J. Veletzos[1]*, Kirty Tiwari[2], Prayash Malla[2], Sweata Sijapati[3], Gokarna B. Motra[4], Kshitij C.Shrestha[4], Dinesh Joshi[5], Heidi Stenner[6], Ido Bruno[7], Arthur Brutter[7], Hari Kumar[8]

[1] Department of Civil Engineering, Merrimack College, North Andover, MA, USA
[2] National Society for Earthquake Technology, Kathmandu. Nepal
[3] GeoHazards International, Kathmandu, Nepal
[4] Department of Civil Engineering, Institute of Engineering, Lalitpur. Nepal
[5] GeoHazards International, Mahendranagar, Nepal
[6] GeoHazards International, Pleasanton, CA, USA
[7] Dept. of Industrial Design, Bezalel Academy of Arts and Design, Jerusalem, Israel
[8] GeoHazards International, Delhi, India

Abstract

This paper describes the results of a dynamic shock table test of an unreinforced stone masonry mock-up building. The primary objective was to study the dynamic characteristics and collapse mechanism of the walls in the out-of-plane direction. The test setup utilized a 3.6m x 6.0m shock table and a two-sided unreinforced stone masonry building mock-up with a slate roof. The walls were constructed of 0.45-m-thick, unreinforced stone masonry with mud mortar, and the roof comprised timber beams, bamboo planks and strips, mud filling, and slate shingles. The shock table test set-up uses a 2070 kg pendulum to impart dynamic shock loads to the table. The roof and walls were connected to ensure they moved together and collapsed with a single shock. The loading protocol involved seven shocks, ranging from 5 to 33 degrees of pendulum swing, and was designed to build damage gradually and culminate in full collapse. Data was collected through video recordings and six accelerometers. While the first three shocks produced minimal damage to the building despite modest accelerations, by the end of the sixth shock, both walls exhibited large vertical cracks. The last shock caused complete collapse of the building and imparted accelerations exceeding 5g to the table and 1.01g to the wall. The test results describe the dynamic characteristics of the walls, damage progression in the walls and the observed damage during a building collapse. This experiment shows that while a single horizontal shock differs from continuous ground shaking experienced in an actual earthquake the results of dynamic shock table tests are a valuable tool in understanding the seismic behaviour of unreinforced stone masonry building.

Keywords: Stone masonry; Dynamic characteristics; Shock table test; Damage patterns; Out-of-plane collapse.

1. Introduction

Unreinforced stone masonry (URSM) buildings with mud mortar are common throughout rural Nepal and are among the most seismically vulnerable construction types. Past earthquakes, including the 2015 Gorkha event, have shown that these buildings often fail through out-of-plane wall collapse, driven by weak mortar, poor wall interlocking, and heavy roof systems. While in-plane behavior of URSM walls has been widely studied, experimental data on out-of-plane dynamic response remain limited, particularly for full-scale buildings representative of traditional construction. Most available studies use small specimens or modified materials that do not reflect actual field conditions. To address this gap, a full-scale dynamic shock table test was conducted on a two-walled stone masonry mock-up with mud–mortar and a slate roof. The experiment simulated horizontal inertial loading to

*Corresponding author: Marc J. Veletzos
Department of Civil Engineering,
Merrimack College, USA
Email: veletzosm@merrimack.edu
https://doi.org/10.3126/jsce.v13i1.89515

observe crack formation, stiffness degradation, and collapse progression under increasing shock intensity. The results provide insight into the dynamic properties and failure mechanisms governing out-of-plane wall behavior.

1.1. Dynamic Shock Table Test

The primary objective of this study was to characterize the out-of-plane dynamic response and collapse behaviour of unreinforced stone masonry walls with mud mortar under transient horizontal shocks. Specific goals were to:

- Document the out-of-plane wall damage leading to collapse.
- Quantify changes in natural frequency and damping ratio as wall damage progressed.
- Examine the influence of roof–wall interaction on wall stability.
- Provide experimental benchmarks for future analytical modelling and seismic strengthening strategies.

1.2. Experimental Test Set-up and Construction Details

Dynamic physical testing was performed using the 3.6 m wide by 6.0 m long shock table testing facility at the Institute of Engineering, Pulchowk Campus of Tribhuvan University in Nepal. Figure 1 shows the general layout of the test set-up, which includes a mock-up of a two-sided classroom with slate roof and a total of six school desks. A dynamic load was imparted to the table by a 2070 kg pendulum which was pulled back and released. The two-walled mock-up

Figure 1. General layout of the test set-up

classroom was constructed of 0.45-m-thick, unreinforced, stone masonry walls with mud mortar. The roof was constructed with timber beams, bamboo planks and strips, mud filling, and slate shingles (see Figure 2 and 3). This building type was selected as it is the most vulnerable building type. The roof and walls were connected with timber keys in three locations on each wall and tied together with galvanized wire. This detail was provided to ensure the roof and top of the walls moved together and the whole building collapsed with a single shock from the pendulum. The roof mass was estimated to be 2210 kg, and the wall mass was estimated to be 7650 kg per wall (15300 kg total for both walls). Steel angles were bolted to the shock table on both sides of the base of each wall to ensure uniform base shear transfer to the walls. A total of six Earthuake (EQ) Desks were placed on the table to study their behavior during a building collapse (Figure 2). The performance of the EQ Desks in these experiments is presented in a companion paper (Veletzos et al., 2026).

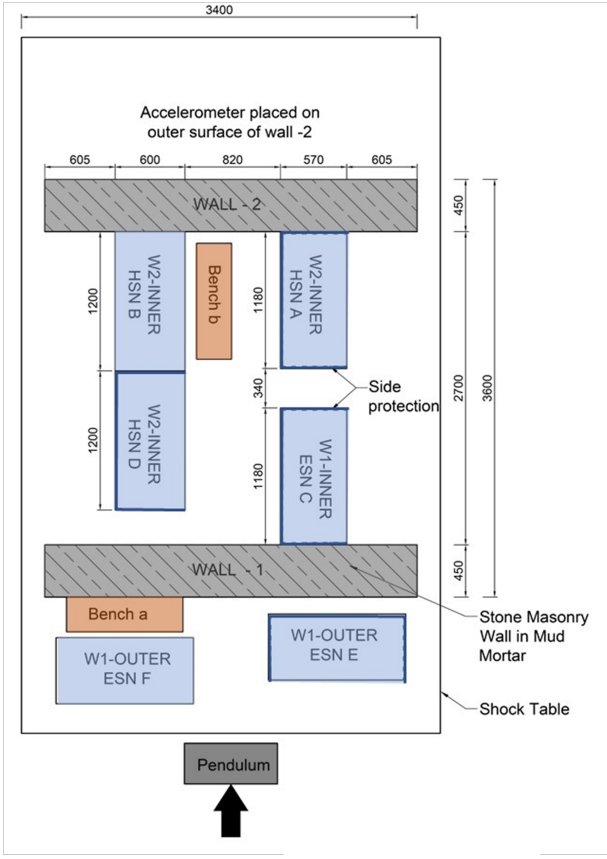

Figure 2. Building mock-up floor plan (note: dimensions are in mm)

1.3. Loading Protocol

The loading protocol was designed to slowly build damage in the wall and culminate in the full collapse of the building due to a single shock. Partial collapse of a wall or roof was not desirable, as a parallel objective was to impart the largest loading on the EQ Desks. Table 1 shows the testing sequence which included a total of seven shocks from the pendulum ranging from 5 degrees to the maximum possible angle of 33 degrees.

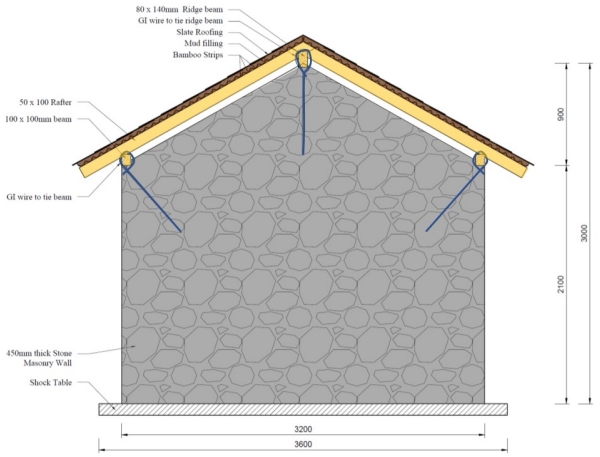

Figure 3. Building mock-up wall and roof details (note: dimensions are in mm)

Table 1. Shock table testing sequence

Shock	Pendulum Angle (deg)
1	5
2	5
3	5
4	7.5
5	10
6	10
7	33

1.4. Data Acquisition

The primary data were collected via video recordings from seven locations outside the building and one location inside the building. In addition to the videos, a total of six accelerometers were installed on or near Wall 2 of the mock-up (Figure 4). One accelerometer was placed on the shock table, three were placed at approximately 1 m height above the table, and two were placed at a height of approximately 1.9 m

Figure 4. Location of the six accelerometers on and near Wall 2

2. Experimental Results

The first three shocks produced little if any damage to the building despite modest accelerations of both the shock table and the wall. During Shocks 4 and 5, an initial vertical splitting crack developed between the two wythes of the wall. This crack gradually widened and became more pronounced through subsequent loading, becoming clearly visible by the end of Shock 6. Results from the first six shocks indicate a gradual progression of damage characterized primarily by the development and growth of this vertical splitting crack. The evolution of damage is also reflected in the changing dynamic characteristics of the system (i.e., natural frequency and damping). Full collapse of the building occurred in Shock #7 and the details of the collapse mechanism are presented in Section 2.3.

2.1. Accelerometer Data Summary

The maximum recorded acceleration of each accelerometer is shown in Table 2. Shock #7 imparted the largest accelerations on the table and the wall and resulted in full collapse of the mock-up building. The magnitudes of the accelerations reduced with height up the wall.

Figure 5 and 6 show the acceleration time histories of Shock #6 and #7, respectively. These figures show a large acceleration from the initial pendulum impact, a modest negative acceleration due to the springs on the far end of the table pushing the table back towards its original position, and a second pendulum impact occurring approximately 1.5 seconds after the first impact. This second pendulum impact occurred because the pendulum bounced off the table after the first impact and then struck the table a second time. Shock #6 imparted accelerations of 1.5g to the table and up to 0.79g to the wall (1g equals the acceleration due to gravity). These are very large accelerations and yet the building remained standing. Shock #7 caused complete collapse of the building and imparted an acceleration beyond the measurable range of the accelerometer (i.e. greater than 5g) to the table and 1.01g to the wall. Figure 7 shows

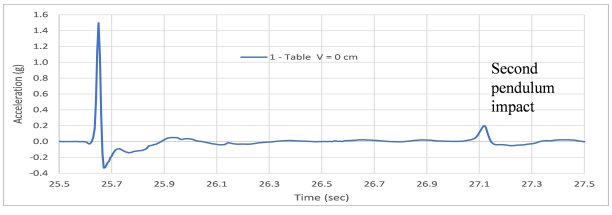

a) Table accelerations

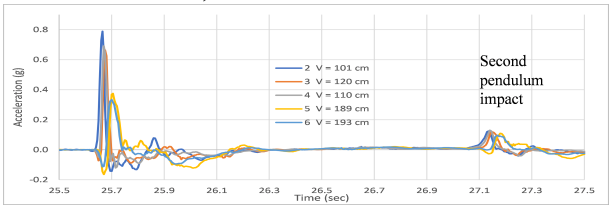

b) Wall accelerations

Figure 5. Shock #6 (10 deg) acceleration time histories

Table 2. Maximum Acceleration at Each Accelerometer

Shock #	Angle (deg)	Accelerometer Number and Height Above Shock Table					
		1 V = 0 cm	2 V = 101 cm	3 V = 120 cm	4 V = 110 cm	5 V = 189 cm	6 V = 193 cm
1	5	0.33	0.23	0.20	0.20	0.17	0.15
2	5	0.26	0.20	0.17	0.18	0.17	0.15
3	5	0.39	0.28	0.25	0.26	0.22	0.20
4	7.5	0.63	0.41	0.37	0.39	0.30	0.24
5	10	1.14	0.67	0.52	0.60	0.39	0.31
6	10	1.50	0.79	0.66	0.69	0.38	0.33
7	33	> 5.0*	1.01	na**	0.81	na**	na**

* Acceleration exceeded the measurable range (5 g) of the accelerometer.

** Accelerometer removed prior to collapse to prevent damage.

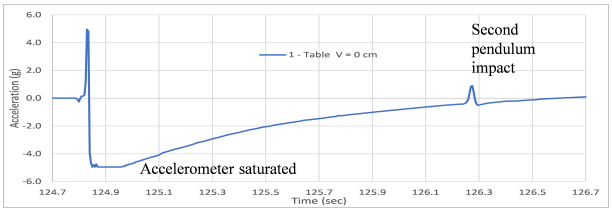

a) Table accelerations

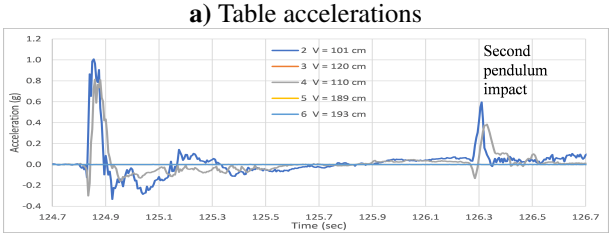

b) Wall accelerations

Figure 6. Shock #7 (33 deg) acceleration time histories

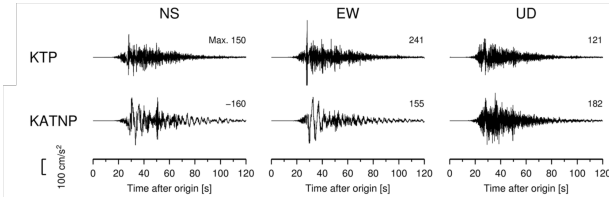

Figure 7. Ground accelerations from the KTP and KATNP stations during the 2015 Gorkha Earthquake (Takai et al., 2016)

ground accelerations from the 2015 Gorkha earthquake. This figure shows a peak ground acceleration of 0.25g in the East-West direction from the "KTP" instrumentation station, which was approximately 75 km from the epicenter. This figure also shows a duration of shaking of approximately 40 seconds. Most stone masonry buildings with mud mortar subjected to the shaking shown in Figure 7 collapsed due to the resonance behavior that developed over the duration of the earthquake. This information is presented to show that a single horizontal shock is not the same as continuous ground shaking from an earthquake and that the accelerations measured in the shock table experiments of this report do not directly correlate with accelerations of actual earthquakes.

2.2. Frequency Response and Frequency Response Functions

Figure 8 shows the Fast Fourier Transform (FFT) of accelerometer sensors #1, #3, and #5 for the first six shocks and illustrates the frequency content of the building's vibrational response. These figures provide a spectral representation of the dynamic behaviour. Figure 9 presents the Frequency Response Functions (FRFs) for the accelerometer sensors for a low-intensity (Shock #1) and a high-intensity (Shock #6) event. The FRF plots are crucial for understanding the building's dynamic characteristics, as they show the relationship between the input frequency from the shock table and the resulting output frequency of the building. The natural frequency of the wall is clealy identified by the peaks on the graphs. The width of these peaks can be used to estimate the damping in the wall.

Table 2 provides a quantitative summary of the building's dynamic properties across multiple shock events. This shows the measured peak response frequency and the corresponding damping ratio for different sensor groups at two different wall heights. The data reveals a consistent trend. As the shock intensity increases from event #1 to #6, the peak response frequency of the building decreases. For example, the frequency drops from 2.48 Hz in Shock #1 to 1.27 Hz in Shock #6. In addition, the damping ratio increases significantly. For sensors #5 and #6, the damping ratio rises from 15% in Shock #1 to 32% in Shock #6. The observed trends indicate a non-linear dynamic response of the stone masonry building to increasing shock intensity. The decrease in the building's natural frequency with more intense shocks suggests that the structure becomes "softer" as it is subjected to greater forces. This change in stiffness could be attributed to the opening of cracks

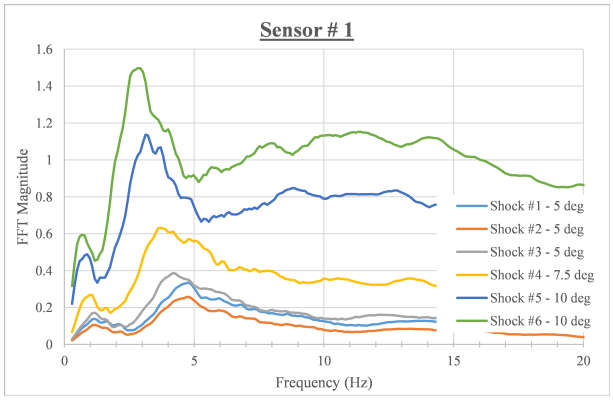

a) Sensor #1 (Table)

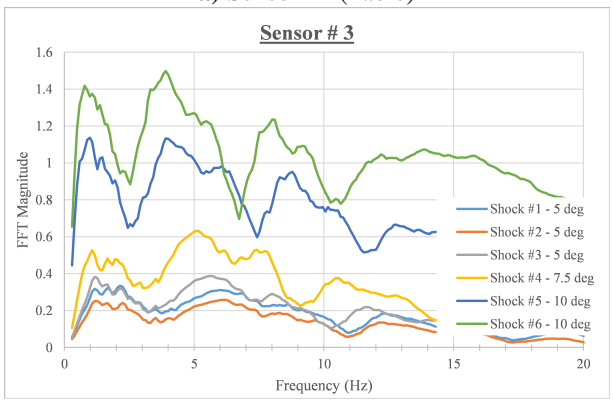

b) Sensor #3

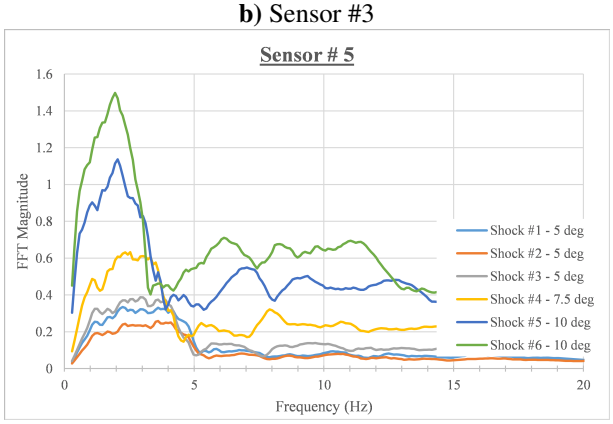

c) Sensor #5

Figure 8. Fast fourier transform of accelerometer sensors

between masonry stones and the non-linear behavior of the mortar joints under higher loads. Simultaneously, the substantial increase in the damping ratio indicates that the building's ability to dissipate energy from the vibrations improves with higher shock intensity. This is an important finding, as increased damping can act as a protective mechanism, preventing an excessive build-up of vibrational energy and mitigating potential damage to the building. This behavior highlights the potential resilience of stone masonry under extreme transient loading conditions if designed with

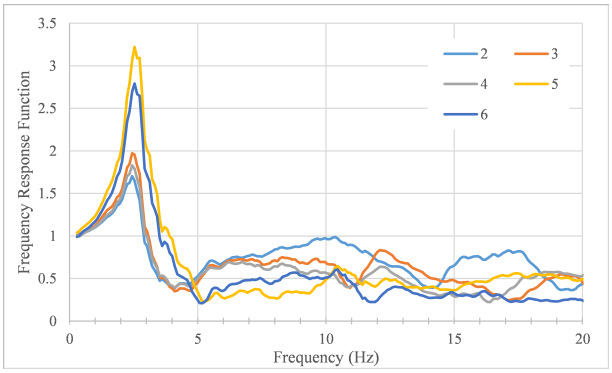

a) Shock #1

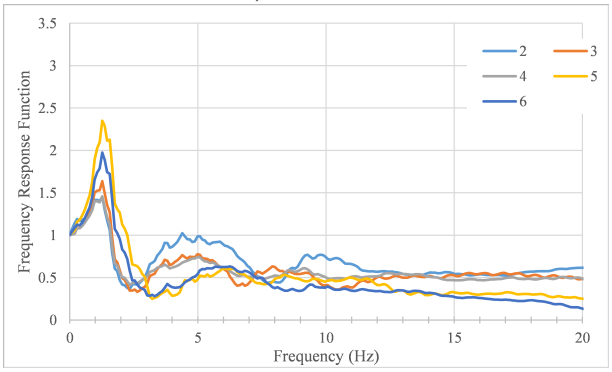

b) Shock #6

Figure 9. Frequency response functions for accelerometer sensors

appropriate seismic details to ensure the walls maintain their structural integrity.

2.3. Damage Progression and Collapse Mechanism

The shock table test demonstrated that unreinforced stone masonry walls with mud mortar fail through a progressive but asymmetric collapse sequence, where initial cracking and separation of the wythes evolve into full structural failure and eventual roof collapse. The first pendulum impact generated vertical cracks that split the wall wythes, and the second impact introduced additional shear forces that widened these separations and destabilized the walls (Figure 10 to 12). Wall 1 then failed: its wythes buckled outward in opposite directions, leading to rapid loss of capacity and ejection of material inward and outward, which in turn triggered roof collapse (see Figure 13). Wall 2, by contrast, initially remained more intact, partly stabilized by its roof–wall connections and interior EQ desks, but eventually began to buckle in portions not directly braced; its final failure occurred as the roof pulled the wall following the collapse of Wall 1 (see Figure 14 and 15). The roof collapse followed wall failure, such that wall and roof debris fell sequentially rather than simultaneously; the ridge beam split, slate shingles were ejected, and the final roof position was partly supported by wall debris and

Table 3. Natural frequencies and damping ratios

Shock #	FRF Peak Response		Damping Ratio	
	Freq. (Hz)	Period (sec)	Sensors 2, 3, 4	Sensors 5, 6
1	2.48	0.40	25%	15%
2	2.46	0.41	20%	15%
3	2.19	0.46	32%	23%
4	1.97	0.51	38%	22%
5	1.43	0.71	53%	32%
6	1.27	0.79	52%	32%
7	Na	Na	na	na

the EQ desks rather than bearing directly on the ground (Figure 16 and Figure 17). These observations highlight that walls constructed with the same materials and details may not collapse in the same manner, and that local crack development, roof–wall interaction, and interior placement of furniture may influence the damage progression and collapse mechanism.

Figure 10. Initial pendulum impact (Shock #7) generates shear in walls and produces vertical crack separating the wall wythes

Figure 11. Second pendulum impact (Shock #7) produces additional shear in the walls and further separates wall wythes.

3. Conclusion

The shock table test results demonstrate a clear and significant non-linear out-of-plane response in an unreinforced stone masonry mock-up building. As the

Figure 12. Contact of desks A and B with Wall 2 temporarily stabilizes wall interior wall wythe of wall 2. portion of wall 2 NOT in contact buckles.

Figure 13. Wall 1 wythes buckle in opposite direction. Wall 1 loses load bearing capacity. Roof begins to fall. Roof-wall connections hold wall 2 together (somewhat).

intensity of the seismic shocks increased, the building's natural frequency decreased, while its damping ratio increased. This indicates that the structure becomes more flexible and more capable of dissipating energy under higher-intensity loading, highlighting its potential for resilient behavior if the walls are sufficiently confined to maintain structural integrity.

The shock table test demonstrated that the unreinforced stone masonry walls failed through progressive cracking and buckling of the wythes, followed by roof collapse. Wall 1 exhibited a more sudden failure with explosive outward buckling and rapid ejection of material, while Wall

Figure 14. Roof over wall 1 collapses. wall 2 loses load bearing capacity.

Figure 15. Wall 2 collapses.

Figure 16. Collapse of wall 2 continues.

Figure 17. Roof impact splits the roof along the ridge beam and causes slate roofing to fly off.

2 collapsed somewhat more gradually, its failure closely tied to the roof's lateral and downward pull. These observations highlight the potential variability of out-of-plane collapse mechanisms in stone masonry walls with mud mortar and underscore the influence of construction detailing, roof–wall interaction, and potentially localized interior support from furniture on overall collapse behavior. Future research should examine how modest confinement or roof-to-wall strengthening can delay or prevent wythe separation, thereby improving the seismic resilience of traditional stone masonry buildings.

References

Takai, N., Shigefuji, M., Rajaure, S., Bijukchhen, S., Ichiyanagi, M., Dhital, M. R., & Sasatani, T. (2016). Strong ground motion in the kathmandu valley during the 2015 gorkha, nepal, earthquake. *Earth, Planets and Space*, *68*(10). https://doi.org/10.1186/s40623-016-0383-7

Veletzos, M. J., Sijapati, S., Malla, P., Tiwari, K., Joshi, D., Stenner, H., Bruno, I., Brutter, A., Kumar, H., Motra, G. B., Shrestha, K. C., & Cedillos, V. (2026). Investigating the protective capabilities of earthquake desks through compression and shock table tests. *Proceedings of the 4th International Conference on Earthquake Engineering and Post Disaster Reconstruction Planning (ICEE-PDRP 2026) (Unpublished)*.

This page is intentionally left blank.